Section 2
ADVANCED TECHNOLOGY DEVELOPMENTS

2.A Laser Patterning of Y-Ba-Cu-O Thin-Film Circuits

In this article studies on electrical properties of Y-Ba-Cu-O test circuits fabricated using a laser-patterning technique are reported. Laser patterning implements a focused beam from a cw Ar-ion laser to selectively heat up an epitaxial Y-Ba-Cu-O film in a controlled (oxygen or oxygen-free) atmosphere. Local heating enables oxygen to diffuse in or out (depending on the outside atmosphere) of the laser-annealed lines and form oxygen-rich (superconducting) regions next to oxygen-depleted (insulating at low temperature) ones. The procedure is noninvasive, does not require a patterning mask, and does not contaminate or damage the surface of patterned films. Our laser-written, oxygen-rich lines (typically 4 mm to 60 mm wide) possess excellent superconducting properties with zero resistivity at 90 K and critical current densities of above 2 MA/cm^2 at 77 K. On the other hand, oxygen-poor regions are semiconducting and exhibit at low temperatures thermally activated transport, well described by a three-dimensional, variable-length hopping process. Their resistance below 100 K is above 10 MW/square. A number of test structures patterned by laser writing, such as a microbridge, coplanar transmission line, open-ended microwave resonator, photoconductive switch, and Y-Ba-Cu-O field-effect transistor, have been presented.

Planar patterning of YBa2Cu$_3$O$_{7-x}$ (YBCO) thin films is one of the key technological issues that must be resolved before successful fabrication of even moderately complex, high-T_c superconducting circuits will be possible.[1] YBCO is a multielement material with highly anisotropic crystalline structure,

which makes the etching process difficult and often results in patterns with fuzzy edges and a degraded (e.g., oxygen-deficient) chemical composition. The problem is especially important in few-micron-wide circuits intended for very high current density and/or high-frequency applications since damaged, oxygen-depleted edges severely limit the structure's supercurrent-carrying capabilities and produce excessive RF losses.[2] In addition, the YBCO surface is extremely sensitive to contamination by chemicals used in standard patterning procedures.

Micropatterning techniques, suitable for YBCO thin-film circuits, usually represent a combination of photolithography and various wet/dry-etching processes.[1] So far, the most successful is ion milling, which allows one to fabricate structures with submicrometer dimensions. Unfortunately, the ion-milling process requires a photomask and expensive vacuum equipment, and it often leads to patterns with partially oxygen-depleted edges. Laser ablation is also a convenient dry-etching technique. The method is fast and requires no patterning mask or any protection of the YBCO surface. However, it produces patterns "sprinkled" with ablated debris, and its practical applicability is limited to rather simple and undemanding structures.[3]

Recently a new laser method for patterning YBCO circuits was demonstrated.[4–8] The technique is based on the observation that YBCO electrical and optical properties are very sensitive to the material's oxygen content. Oxygen can be diffused in or out of the YBCO film by heating the sample in either the presence or the absence of an oxygen atmosphere. The heating can be done locally with a focused laser beam. Thus, an intentionally oxygen-depleted (insulating at low temperatures) YBCO film can be patterned by embedding in it oxygen-rich (superconducting) lines or vice versa. The writing is fully reversible, and the patterns can be either erased by furnace annealing or rewritten by subsequent laser writing. Most importantly, the technique is noninvasive, requires no patterning mask, and results in completely planar structures, free of surface contamination or edge degradation.

The aim of this article is to demonstrate that the laser-writing method is a reliable and practical technique, perfectly suited for patterning even complicated YBCO thin-film devices and circuits. We examine several laser-written test devices and show that they exhibit excellent superconducting properties and can survive, without degradation, long-term storage in air at room temperature. Some of them also combine in a new and unique way the superconducting and dielectric properties of the oxygen-rich and oxygen-poor YBCO phases. These latter structures are, in our opinion, prime candidates for the proposed high-T_c superconducting optoelectronics.[9]

Figure 56.12 presents a block diagram of our laser-patterning apparatus. The system consists of an Ar-ion cw laser (λ = 0.514 mm), shutter, focusing microscope, and computer-controlled X-Y translational stage with a gas chamber and sample holder. The sample ambient atmosphere is either pure nitrogen or oxygen. Contrary to our previous arrangement,[8] the substrate of the YBCO film is not in a direct heat contact with the metallic substrate holder, but it is suspended on a thin thermal insulator. This change allowed us to reproducibly write two-dimensional patterns not only on YBCO-on-$LaAlO_3$ films but also on films

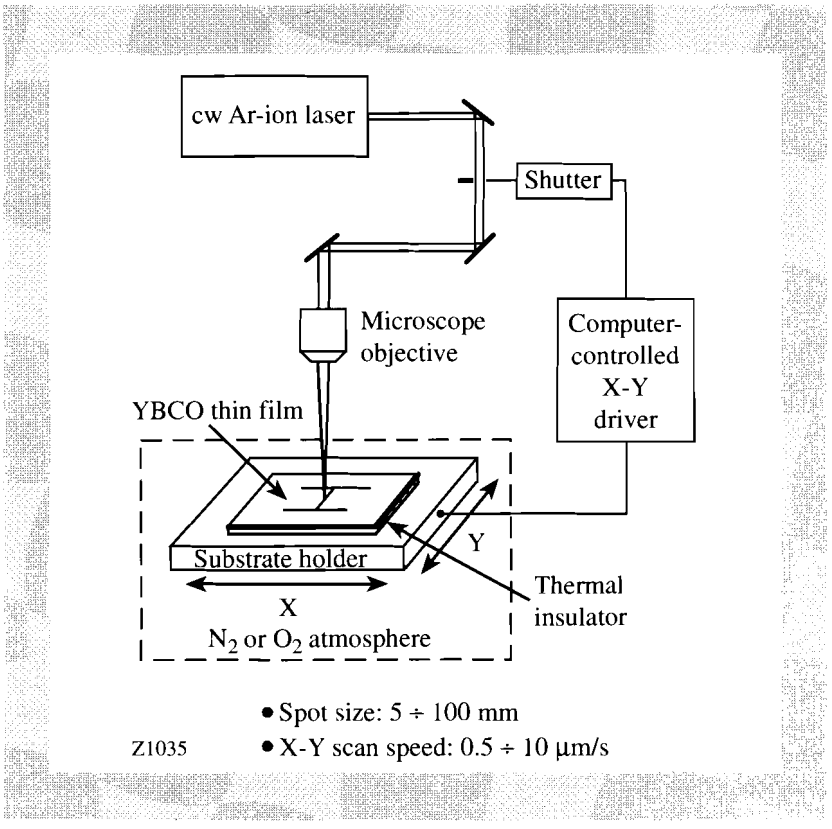

Fig. 56.12
Block diagram of a two-dimensional laser-patterning apparatus.

deposited on MgO and $SrTiO_3$. Simultaneously, it eliminated the previously considered need to implement a substrate heater. Typical line dimensions of our patterns varied from <5 μm to 100 μm. Laser-power intensity applied to the film was kept between 0.2 and 5 mW/μm^2, and a translational stage speed was in the range of 0.5 to 5 μm/s for writing oxygen-rich lines and ~50 μm/s for (written in nitrogen) oxygen-poor structures.

Our test structures were laser patterned on about 200- to 300-nm-thick epitaxial YBCO films, grown using a single-target RF sputtering technique.[10] The best as-deposited films exhibited about 0.5-K-wide (10%–90%) superconducting transition ΔT_c with the zero resistivity T_{c0} at 89.5 K, and the critical current density J_c of above 2 MA/cm^2 at 77 K. The films have been intentionally deoxygenated by radiative heating for 60 min in 15 mTr of argon at 680°C to become nonsuperconducting. Indeed, after the argon annealing, their sheet resistance below 100 K was above 10 MΩ/square, which represented the upper limit of our resistance-measurement apparatus. Figure 56.13(a) shows the resistance-versus-temperature $R(T)$ curve for one of our oxygen-depleted films. We see that the film resistance rapidly increases at low temperatures, quickly reaching our 20-MΩ measurement limit. The observed behavior is characteristic for a thermally activated transport in disordered semiconductor materials, as illustrated in Fig. 56.13(b), where the $\ln[R(T)/R(300\ \mathrm{K})]$ dependence is plotted as a function of the fourth root of the inverse temperature. We note that most of our experimental data points follow a straight line, demonstrating that the low-temperature transport in oxygen-poor YBCO is controlled by three-dimensional, variable-length hopping.[11]

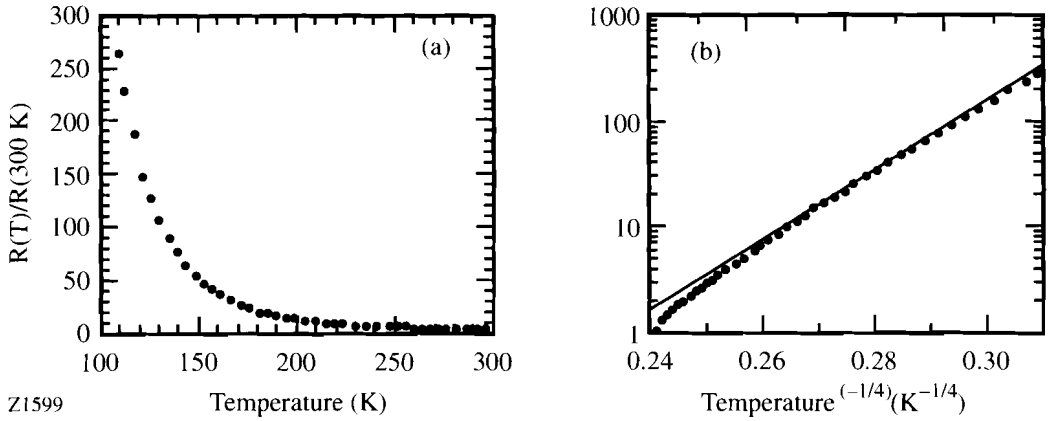

Fig. 56.13
Resistive behavior of an ~200-nm-thick YBCO-on-$LaAlO_3$ film. (a) Linear $R(T)/R(300\ K)$ dependence and (b) logarithmic $R(T)/R(300\ K)$ dependence versus the fourth root of the inverse temperature. The film room temperature resistance $R(300\ K) \approx 75\ k\Omega$.

Optical micrographs of four laser-written test structures are shown in Fig. 56.14. All devices are fully monolithic and exhibit very sharp (less than 1 μm wide) superconducting-semiconducting interfaces with linear current-voltage characteristics.[12] Figure 56.14(a) shows a 7-μm-wide microbridge designed for ultrafast optical response measurements,[9,13] as well as for $R(T)$ and $J_c(T)$ tests as discussed later. Figure 56.14(b) presents a 10-μm-wide, oxygen-poor YBCO photoconductive switch incorporated into a coplanar transmission line. The structure is similar to that of a GaAs photoconductive switch (so-called "Auston switch"), routinely used in generating ultrafast electrical transients,[14] and is intended for our studies of the dynamics of electron-hole pair generation in semiconducting YBCO. It is also expected to find applications as an electrical pulse generator in HTS optoelectronic circuits.[10] Figure 56.14(c) shows one end of an open-ended coplanar microwave resonator. The resonator is incorporated

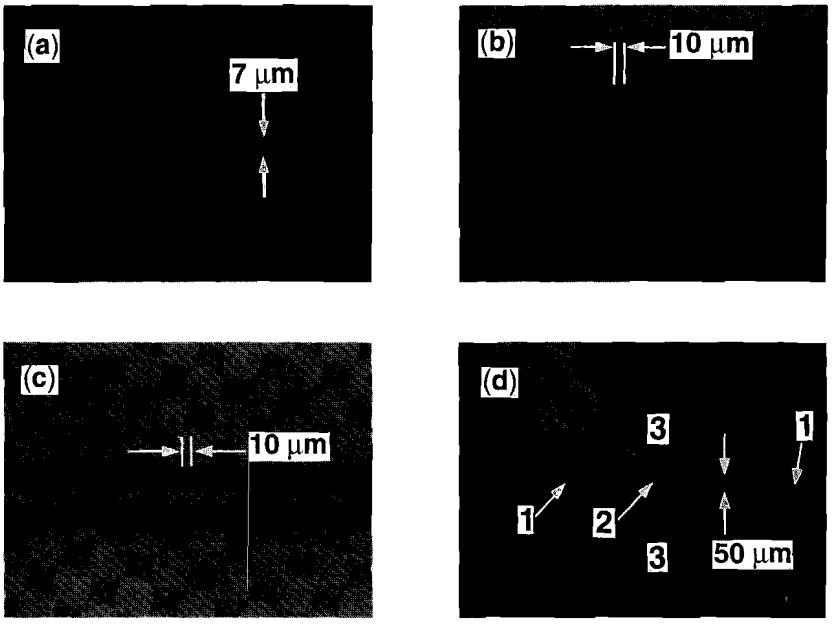

Fig. 56.14
Optical transmission micrographs of oxygen-rich (dark) test structures, laser written on oxygen-depleted (semitransparent) YBCO films. (a) 7-μm-wide and 160-μm-long microbridge; (b) 10-μm-wide oxygen-poor photoconductive switch incorporated into a superconducting coplanar transmission line; (c) left end of an open-ended coplanar microwave resonator; and (d) field-effect test structure prepared in a single YBCO film (gate electrode not shown).

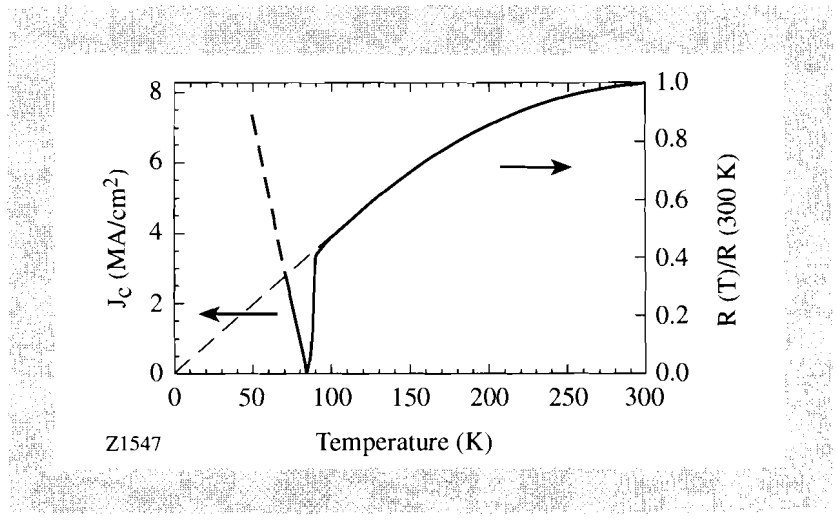

Fig. 56.15
Resistance and critical current density dependence on temperature for the microbridge shown in Fig. 56.14(a).

into a coplanar transmission line. Its 10-μm-wide coupling slit was patterned by overwriting the oxygen-rich line in N_2 atmosphere. A resonator structure identical to that shown in Fig. 56.14(c) but with the line separation of 285 μm has been tested and has shown very good microwave properties. Its quality factor measured at 24 K was about 5000 at 6.5 GHz, and we observed more than 60-dB improvement in the coplanar-line-transmitted power S_{21} in the frequency range of 1 to 15 GHz, as the temperature was lowered from 300 K to that below T_c. At all temperatures below T_c, the S_{21} was near 0 dB, indicating low microwave losses of the oxygen-poor YBCO.[15] These findings clearly demonstrate applicability of our laser-patterning technique for fabricating microwave circuits and devices. Finally, Fig. 56.14(d) presents a top view of a YBCO electric-field device with a partially deoxygenated channel. The homogeneous regions with three different levels of gray, visible in this figure, correspond to (1) highly oxygenated drain and source (the two dark regions; $T_c \approx 90$ K), (2) partially deoxygenated ($T_c \approx 25$ K), 1-mm-long, 60-mm-wide channel, and (3) insulating (semitransparent) transistor borders. Our preliminary measurements indicated a presence of the charging effect in the above structure and showed that in thick YBCO films (~200 nm in our case), field-induced modulation of J_c, rather than T_c, is more likely to be observed.[16]

The electrical [$R(T)$ and $J_c(T)$] measurements of our test structures were performed in the standard four-probe geometry using a temperature-controlled, computer-driven station. The sample electrical contacts were wire bonded to 300-nm-thick, silver contact pads evaporated directly on top of the oxygen-rich lines. Figure 56.15 shows the $R(T)$ and $J_c(T)$ curves measured for the microbridge presented in Fig. 56.14(a). We note very good superconducting properties of our laser-patterned line. The somewhat unconventional shape of the $R(T)$ dependence is due to the fact that at high temperatures there is a finite contribution from the oxygen-poor YBCO, which is parallel to the microbridge and fills the space [see Fig. 56.14(a)] between the two oxygen-rich contacts. At low temperatures (below 150 K) the resistance decreases linearly since in this temperature range, the resistivity of the oxygen-poor material is very high (see Fig. 56.13). The low-temperature extrapolation of the $R(T)$ curve crosses the resistance axis at the axis origin. The $J_c(T)$ dependence is almost linear, and J_c increases at the rate of about 0.2 MA/cm^2/K, reaching above 2 MA/cm^2 at 77 K.

Figure 56.16 shows in detail the resistive transition presented in Fig. 56.15 (sample W.2-43-A42, open squares), together with the transitions recorded for a laser-written line fabricated on a magnetron-sputtered YBCO-on-$SrTiO_3$ film (sample UR 168, open squares) and for the corresponding original, as-deposited films (samples W.2-43-A42 and UR 168, closed squares). Comparing the two sets of curves we note that in both cases the laser-patterned lines and the original films exhibit the same ΔT_c and T_{c0}; thus, a somewhat depressed T_c, observed in the UR 168 sample, should not be associated with the oxygen deficiency but is, apparently, due to the film's non-optimal Y:Ba:Cu cation ratio, or large concentration of defects. The observed differences between the $R(300\text{ K})/R(100\text{ K})$ ratios for the laser-written lines and the original films are due to the finite contribution of the semiconducting YBCO to the actual $R(T)$—as we mentioned before—explaining the shape of the $R(T)$ presented in Fig. 56.15.

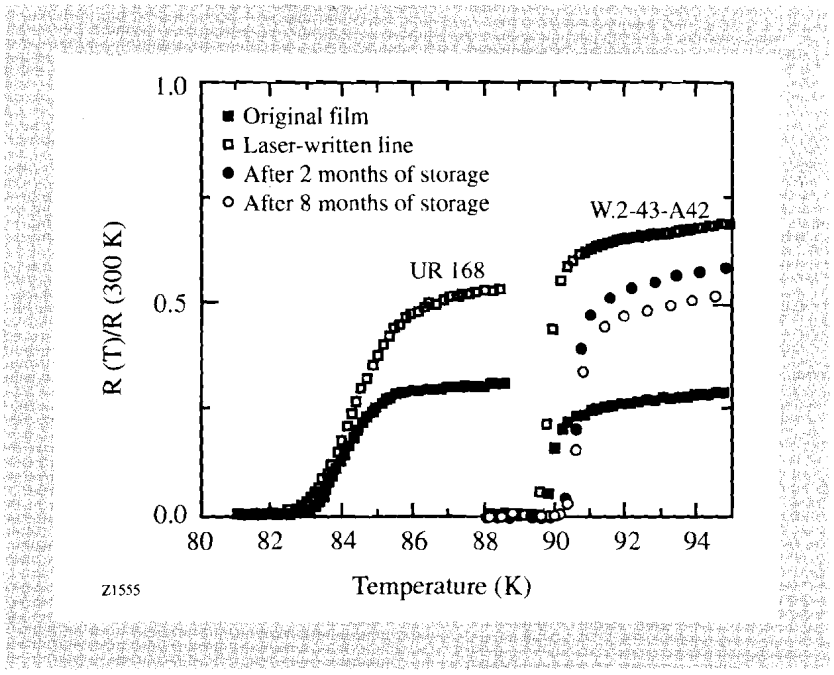

Fig. 56.16
Comparison between the superconducting transitions of oxygen-rich laser-written lines (open squares and open and closed circles) and the original superconducting films (closed squares). UR 168 denotes the 80-nm-thick film deposited on $SrTiO_3$, while the label W.2-43-A4 corresponds to the 280-nm-thick YBCO-on-$LaAlO_3$ film. Traces for the laser-written pattern on the W.2-43-A4 film were taken on the same sample right after the laser-patterning process (open squares), as well as two (closed circles) and eight (open circles) months later.

Figure 56.16 also presents two $R(T)$ traces (open and closed circles) measured on the same W.2-43-A42 sample, but two and eight months after the original patterning. During that time our sample was kept at room temperature and exposed to air. We note that instead of expected degradation in the sample's superconducting properties, the laser-written structures actually exhibit slightly *enhanced* T_{c0}'s and improved $R(100\text{ K})/R(300\text{ K})$ ratios. We associate these effects with a slow process of long-term oxygen ordering, which should lead to the film's "self-improvement." The storage did not lead to any visible changes in the physical appearance of our samples. The superconducting-semiconducting interfaces, as observed under optical and scanning electron microscopes (not shown), remained less than 1 μm wide. The long-term stability of the superconducting and structural properties of our samples demonstrates that, indeed, laser writing is a practical technique for patterning YBCO films.

In conclusion, we have demonstrated that laser patterning can be successfully used to fabricate practical YBCO thin-film devices and circuits. The technique

produces well-defined patterns with undamaged crystalline structure and very sharp (less than 1 μm wide) interfaces. The writing is fully reversible, and the patterns can be either erased by furnace annealing or rewritten by subsequent laser writing. Most importantly, the technique is noninvasive, requires no patterning mask, and results in completely planar, free-of-surface contamination structures. The laser-patterned structures are characterized by superconducting properties, which are as good as those of the original superconducting films, even after many months of shelf storage. We presented a number of completely monolithic test structures that were all fabricated using laser patterning. The devices are intrinsic to the YBCO material (they cannot be reproduced using, e.g., metallic superconductors), and they demonstrate, in our opinion, that laser patterning can be successfully implemented in fabricating a variety of electronic and optoelectronic, high-T_c devices. The technique is especially promising in the YBCO-based optoelectronics since, in this compound, both electrical and optical properties are very sensitive to the sample's oxygen content.

ACKNOWLEDGMENT

The authors would like to thank Professor M. R. Beasley for a very helpful discussion regarding variable-distance hopping. This work was supported by the Air Force Office for Scientific Research grants F49620-92-J-0075 (Rochester) and F49620-91-C-0034 (Westinghouse). Additional support was provided in part by the Polish Government grant 2-04979-1 and the Laboratory for Laser Energetics' Frank Horton Graduate Fellowship Program.

REFERENCES

1. See, e.g., A. I. Braginski, in *Superconducting Devices and Their Applications*, edited by H. Koch and H. Lübbig, Springer Proceedings in Physics (Springer-Verlag, Berlin, 1992), Vol. 64, pp. 3–18.
2. P. H. Ballentine, A. M. Kadin, and D. S. Mallory, IEEE Trans. Magn. **27**, 997 (1991).
3. See, e.g., P. H. Ballentine, A. M. Kadin, M. A. Fisher, D. S. Mallory, and W. R. Donaldson, IEEE Trans Magn. **25**, 950 (1989).
4. M. Rothschild *et al.*, Appl. Phys. Lett. **52**, 404 (1988).
5. R. R. Krchnavek *et al.*, J. Appl. Phys. **65**, 1802 (1989).
6. R. C. Dye *et al.*, Appl. Phys. Lett. **57**, 1149 (1990).
7. Y. Q. Shen, T. Freltoft, and P. Vase, Appl. Phys. Lett. **59**, 1365 (1991).
8. R. Sobolewski, W. Xiong, and W. Kula, IEEE Trans. Appl. Supercond. **3**, 2986 (1993).
9. R. Sobolewski, in *Superconductivity and Its Applications*, AIP Conference Proceedings 251, New York, NY, 1992, pp. 659–670.
10. J. R. Gavaler *et al.*, J. Appl. Phys. **70**, 4383 (1991).
11. See, e.g., D. K. Ferry, *Semiconductors* (Macmillan Publishing Company, New York, 1991). Detailed presentation of the low-temperature hopping transport in oxygen-depleted YBCO thin films will be presented elsewhere.
12. R. Sobolewski, W. Xiong, W. Kula, and B. McIntyre, accepted for presentation during the 20th International Conference on Low-Temperature Physics (LT-20), Eugene, OR, 4–11 August 1993, and to appear in Physica B (1993).
13. T. Gong, L. X. Zheng, Y. Kostoulas, W. Xiong, W. Kula, K. B. Ucer,

R. Sobolewski, and P. M. Fauchet, to appear in *Ultrafast Electronics and Optoelectronics V*, Springer Series in Electronics and Photonics (Springer-Verlag, Berlin, 1993).

14. D. H. Auston, Appl. Phys. Lett. **26**, 101 (1975).
15. R. Sobolewski, W. Xiong, W. Kula, W. N. Maung, and D. P. Butler, submitted for presentation during the 4th International Superconductive Electronics Conference (ISEC '93), Boulder, CO, 11–14 August 1993, and to be published.
16. W. Kula and R. Sobolewski, accepted for presentation during the 20th International Conference on Low-Temperature Physics (LT-20), Eugene, OR, 4–11 August 1993, and to appear in Physica B (1993).

2.B Fabrication of Foam Shells Overcoated with Plastic Layers

Future ICF capsule designs incorporate thick cryogenic layers of fusion fuel (DT). There are a number of techniques currently under investigation to form these thick fuel layers. One such technique is to use a low-density polymer or aerosol (SiO_2) foam matrix to hold the liquid DT. A collaborative effort was undertaken at the Institute for Laser Engineering (ILE) by researchers from both LLE and ILE to explore methods for fabricating polymer foam capsules. These types of capsules, if successful, will be used for experiments to be conducted on the upgraded OMEGA laser system. This report summarizes the knowledge obtained by LLE from this collaborative effort for fabricating foam shell targets overcoated with a plastic layer. Fabrication of the foam shells is described, followed by a description of the process for overcoating the plastic layer on the foam shell.

Fabrication of Foam Shells

The foam shells are fabricated using the microencapsulation technique developed by Kubo[1] and refined by Takagi *et al.*[2] During this process, the hydrophobic phase consists of a diluted solution of difunctional or multifunctional monomer. After forming shells from this hydrophobic phase, the monomer is polymerized to form a cross-linked polymer gel. The solvent is removed from the gel to obtain a three-dimensional network structure of low-density foam.

In the Osaka experiments, the W_1, O, and W_2 phases consisted of the composition given in Table 56.II. Fabrication of the foam-shell targets started by mixing 10 g of the O phase and 5 g of the W_1 phase in a 20-ml beaker. The mixture was shaken to form an emulsion of the desired size. The mixture was then poured into a beaker containing 500 ml of the W_2 phase, at a temperature of 45°C, and stirred. The polymerization reaction proceeded for 2 h at 90°C. Upon conclusion

Table 56.II: Composition of the W_1, O, and W_2 phases.

W_1 phase	0.05% aqueous solution of polyoxymethylene sorbitan monopalmitate
O phase	2%–5% of trimethylol propane trimethacrylate (TMPT), 1:1 mixture of diethyl phthalate and di-n-butyl phthalate, 2, 2′ izobis-isobutylonitrile (AIBN) as a polymerization initiator (10% of TMPT), and 0.1%–0.5% of sorbitan monopalmitate
W_2 phase	5%–12.5% of PVA solution in water (DP of PVA: 500)

of the reaction, the O phase had completely gelled. The whole system was washed gently with water several times, and the shells were gently introduced into a beaker containing 100 ml of toluene. The water separated to the bottom of the beaker and was removed using a pipette. The shells settled to the bottom and about 2/3 of the toluene was decanted; 1,2 dichloroethane was then added. Solid spheres and the broken shells sank to the bottom, and the good shells floated on top since they are buoyant in 1,2 dichloroethane due to the encapsulated water. The good shells were collected in ethanol using a pipette, and the ethanol replaced the water inside the shells.

The foam shells were characterized while they were both immersed in ethanol and in a dry state. (A few of the shells in ethanol were dried using a CO_2 critical-point drying method.) Figure 56.17 shows a microscopic image of a foam shell in ethanol. The foam wall thickness is 120 μm, and the concentricity is very good. The outer diameter of the shell is 800 μm. A typical batch contains shells having a wide range of sizes and wall thicknesses that encompass the range of interest for OMEGA Upgrade experiments. In general, the wall thickness depends more on the concentration of PVA in the W_2 phase, and less on the concentration of TMPT in the O phase. Figure 56.18 shows the effect of the PVA concentration on the wall thickness. Since any given batch of foam shells contains shells with a wide range of sizes and wall thicknesses, Fig. 56.18 should be interpreted qualitatively. The cell structure of the foam is shown in Fig. 56.19. The cell size ranges from less than one to a few microns. It is not known at present what controls the cell size. Different compositions of the O phase may give different cell sizes and structures; the effect of this composition will be studied later. Figure 56.20 shows the surface structure of a dried foam shell. The density of the surface appears greater than that of the bulk of the foam, possibly due to an interfacial effect between the O phase and the W_2 phase. That is, the chain conformation of the polymerized TMPT at the interface may not be Gaussian, as it is in the bulk, particularly in the direction perpendicular to the interface. As a result, the density of the chains at the interface becomes higher than that inside the bulk. The density of the foam shells was determined by measuring the weight of each shell with a microbalance and measuring their corresponding diameter and wall thickness. The density of ten shells was measured and its mean was calculated. The shells were from a batch made using a 3% TMPT solution and a 2.5% PVA solution. The average foam density was 57.9 mg/cm^3 with a standard deviation of 5.0 mg/cm^3. The density measured is generally higher than that calculated from the concentration of TMPT. This discrepancy is considered to arise from the contraction of the shell during the drying process.

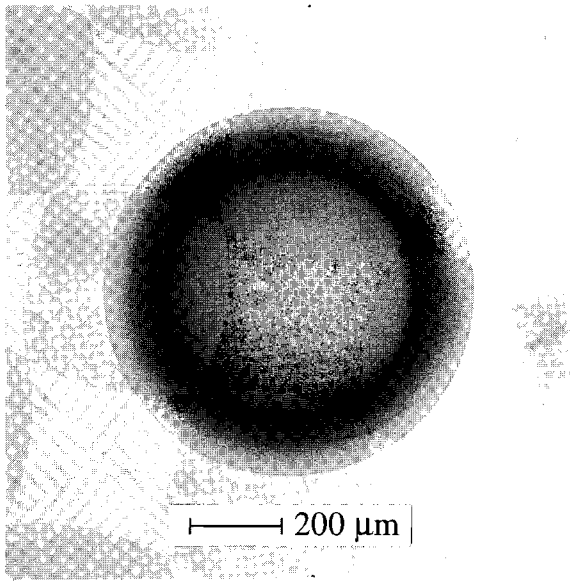

Fig. 56.17
Optical micrograph of a foam shell immersed in ethanol.

T1170

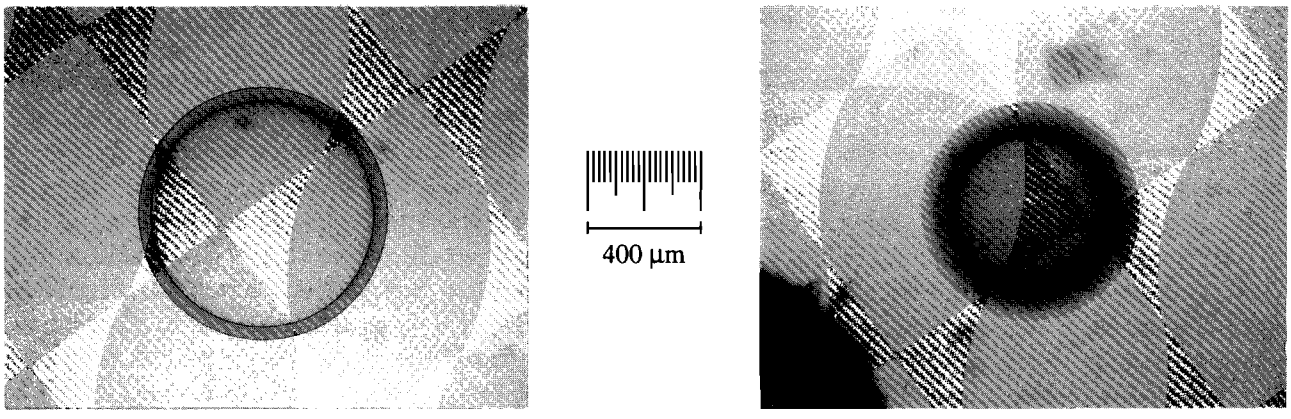

T1126

Fig. 56.18
Effect of PVA concentration in the W_2 phase on the wall thickness of foam shells.

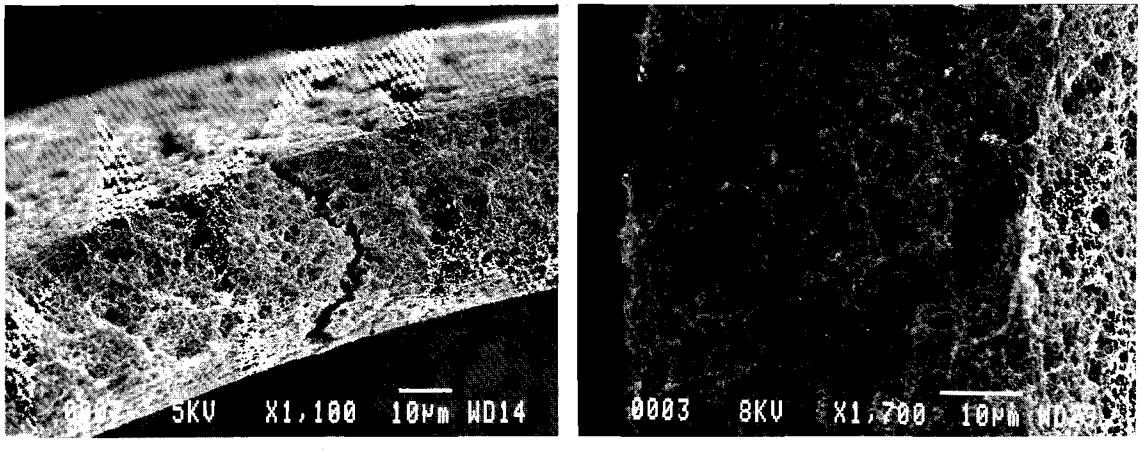

T1128

Fig. 56.19
SEM photos of a fracture cross-section of a foam shell.

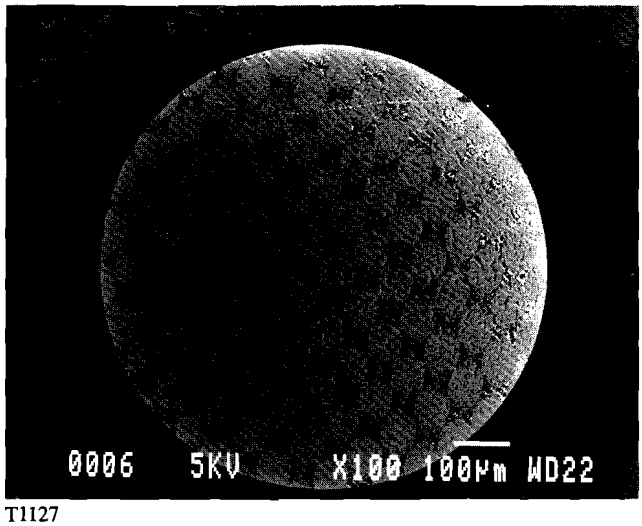

T1127

Fig. 56.20
SEM photo of the outer surface of a dried foam shell.

Fabrication of Plastic-Layer-Overcoated Foam Shells

Overcoating foam shells with a plastic layer is performed by the interfacial polycondensation method.[3] In this method, two reagents dissolved in separate phases that are immiscible in each other react to form a condensed polymer layer that is not soluble in either phase. In the experiments performed at Osaka, hydroxy ethyl cellulose in the W_2 phase and isophthaloyl chloride in the O phase react at the interface of the O phase and the W_2 phase (the outer surface of the foam shell) to form cross-linked hydroxy ethyl cellulose. This method, combined with the microencapsulation technology, produced a polymer layer overcoating on the foam shells.

Figure 56.21 is a schematic showing the polycondensation interfacial polymerization process. Foam shells are impregnated with an oil-soluble reagent, which is dispersed in the matrix of an aqueous solution of another reagent. The two reagents react on the interface to form a cross-linked polymer layer on the foam shells. The foam shells are then collected and dried using a CO_2 critical-point drying method. For this reaction, the shells and the reagents are prepared in the following way. First, the foam shells fabricated previously and stored in ethanol are transferred into *p*-chlorotoluene. A complete replacement of ethanol by *p*-chlorotoluene is necessary, and during the replacement process, care must be taken not to damage the fragile shells. The shells are then transferred into an isophthaloyl chloride solution in *p*-chlorotoluene (concentration of 1 mmol/ml) and kept in this solution long enough to ensure saturation. By mixing this with a PVA solution, the excess *p*-chlorotoluene solution is stripped off leaving only saturated foam shells. The foam shells in the PVA solution are poured into a 2-wt% aqueous solution of hydroxyl ethyl cellulose containing 0.5 wt% of polyoxymethylene sorbitan monopalmitate as a surfactant. The polycondensation reaction does not start until the addition of Na_2CO_3. Since the reaction is reversible, the resulting HCl must be removed to stabilize the reaction. The rate of formation of the plastic layer overcoating was relatively fast, yielding a 7.5-µm layer within 45 min. This reaction forms a flaky surface, which is smoothed by adding NaOH. The whole system is then neutralized by the addition of diluted HCl. The resulting shells are thoroughly washed with water, stored in dioxane, and then dried using the CO_2 critical-point drying apparataus.

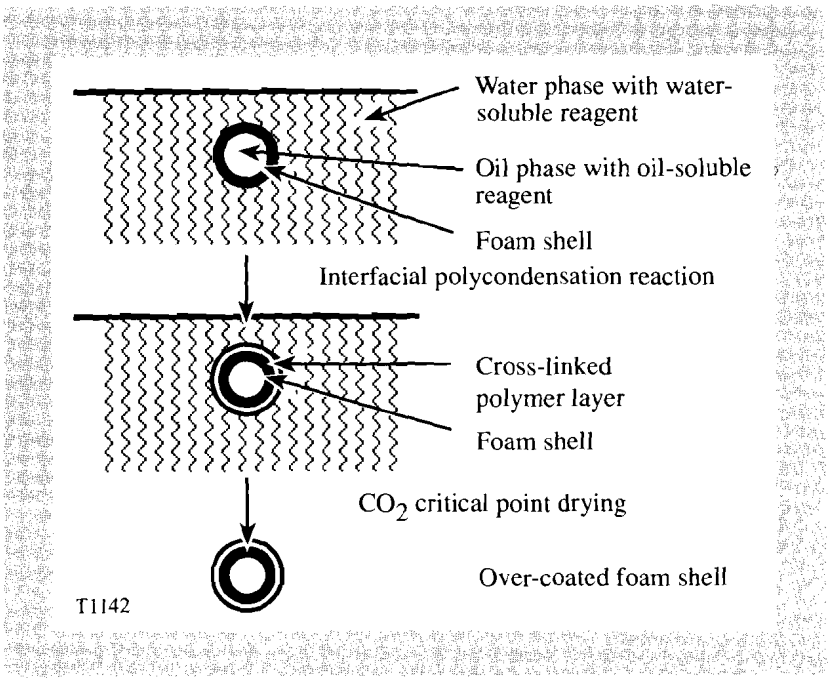

Fig. 56.21
Schematic diagram showing the polycondensation interfacial polymerization process.

Figure 56.22 shows an optical micrograph of the plastic-layer-overcoated foam shell in water. The thickness of the layer can be easily controlled by adjusting the reaction time. A cross-section of the plastic-layer-overcoated foam shell in Fig. 56.23 shows that the adhesion of the plastic layer to the outer surface of the foam shell does not replicate the foam structure, but forms a clean spherical surface. This may be due to the fact that, during the polycondensation reaction process, the interface between the *p*-chlorotoluene-containing shells and the hydroxyl-ethyl-cellulose-containing matrix was always spherical. A scanning electron microscope (SEM) photo in Fig. 56.24 shows that the surface of the plastic overcoating is smooth and void of defects. Furthermore, as previously described, any defects on the surface can be removed by hydrolysis using NaOH.

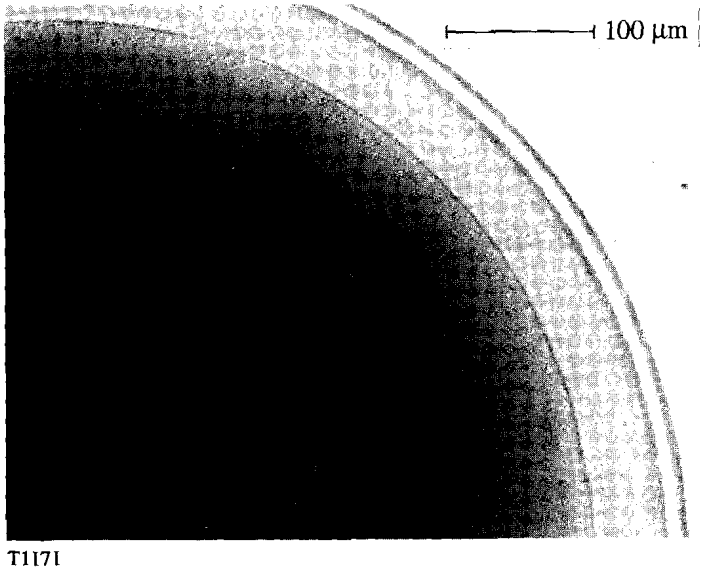

T1171
Fig. 56.22
Optical micrograph of a plastic-layer-overcoated foam shell in water.

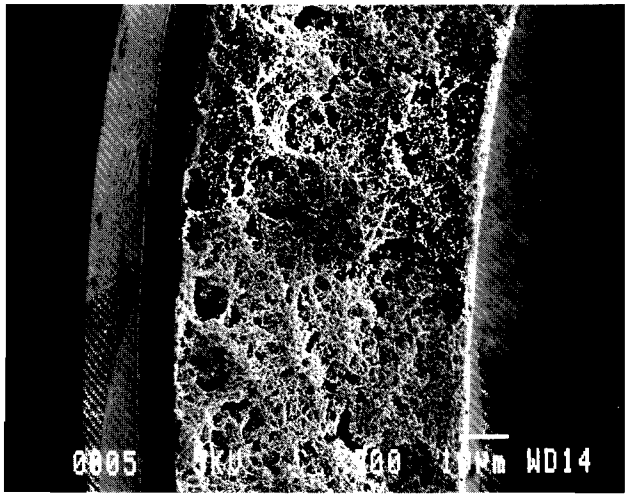

T1136
Fig. 56.23
SEM photo showing a cross-section of a plastic-layer-overcoated foam shell.

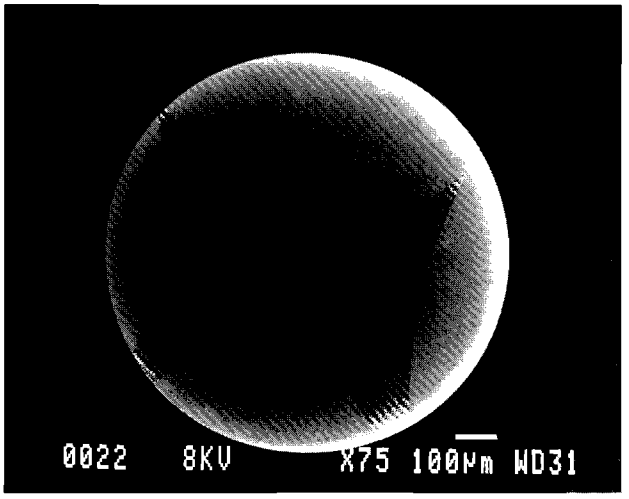

T1135
Fig. 56.24
SEM photo of the surface of a plastic overcoating on a foam shell.

Experience at Osaka University's Institute of Laser Engineering indicates that foam shells with the specifications needed for OMEGA Upgrade experiments can be fabricated using the microencapsulation technique developed at Osaka. It is possible to fabricate plastic-layer-overcoated foam shells having diameters of 0.5–1.5 mm, foam shell thicknesses of 10–120 μm, sphericity and uniformity better than 98%, a foam density of ~50 mg/cm^3, an overcoated-plastic-layer thickness of 3–12 μm, and a plastic layer with an rms surface roughness less than 0.1 μm. The foam density and cell size may be controlled by the proper choice of the chemical composition of the *O* phase during the microencapsulation process. This work remains to be done.

ACKNOWLEDGMENT

It is a great pleasure to acknowledge the hospitality extended to the author during his stay in Japan by Osaka University's Institute of Laser Engineering. He expresses his particular gratitude to Mr. Takagi and Dr. Norimatsu for their assistance and guidance during the course of this work.

REFERENCES

1. U. Kubo and H. Tsubakihara, J. Vac. Sci. Technol. **A4**, 1134 (1986).
2. M. Takagi, T. Norimatsu, T. Yamanaka, and S. Nakai, J. Vac. Sci. Technol. **A(9) 4**, 2145 (1991).
3. E. L. Wittbecker and P. W. Morgan, J. Polym. Sci. **60**, 289 (1959).